

## An integrated microfluidic array system for evaluating toxicity and teratogenicity of drugs on embryonic zebrafish developmental dynamics

Fan Yang, Zuanguang Chen,<sup>a)</sup> Jianbin Pan, Xinchun Li,  
Jun Feng, and Hui Yang

*School of Pharmaceutical Sciences, Sun Yat-sen University, Guangzhou, Guangdong  
510006, China*

(Received 24 February 2011; accepted 8 June 2011; published online 27 June 2011)

Seeking potential toxic and side effects for clinically available drugs is considerably beneficial in pharmaceutical safety evaluation. In this article, the authors developed an integrated microfluidic array system for phenotype-based evaluation of toxic and teratogenic potentials of clinical drugs by using zebrafish (*Danio rerio*) embryos as organism models. The microfluidic chip consists of a concentration gradient generator from upstream and an array of open embryonic culture structures by offering continuous stimulation in gradients and providing guiding, cultivation and exposure to the embryos, respectively. The open culture reservoirs are amenable to long-term embryonic culturing. Gradient test substances were delivered in a continuous or a developmental stage-specific manner, to induce embryos to generate dynamic developmental toxicity and teratogenicity. Developmental toxicity of doxorubicin on zebrafish eggs were quantitatively assessed via heart rate, and teratological effects were characterized by pericardial impairment, tail fin, notochord, and SV-BA distance /body length. By scoring the teratogenic severity, we precisely evaluated the time- and dose-dependent damage on the chemical-exposed embryos. The simple and easily operated method presented herein demonstrates that zebrafish embryo-based pharmaceutical assessment could be performed using microfluidic systems and holds a great potential in high-throughput screening for new compounds at single animal resolution. © 2011 American Institute of Physics.  
[doi:10.1063/1.3605509]

### I. INTRODUCTION

The zebrafish (*Danio rerio*), as a well-established model organism in developmental biology, holds great promise for studying *in vivo* effects of drugs or toxic substances on single individuals.<sup>1</sup> Historically, zebrafish have been used for evaluating the toxicity and teratogenicity of agrochemical and environmental agents.<sup>2</sup> But now, their application in toxic assessment of pharmaceuticals and high-throughput drug screening has been earnestly pursued.<sup>3,4</sup> Accordingly, the zebrafish can be selected as a relevant whole-organism model to perform phenotype-based screenings due in part to its morphological and physiological similarity to mammals.<sup>4</sup>

The embryos, as the early life stage of zebrafish, are particularly susceptible to chemicals, and they are the most inaccessible in the conventional mammalian models for toxic assessment.<sup>5</sup> Recently, increasing attention has been paid to the zebrafish embryos because of their remarkable merits including the transparent trait, large numbers in a clutch, cost effectiveness, and lacking ethical concerns due to immature perception of pain comparable to adults. For these reasons,

---

<sup>a)</sup>Author to whom correspondence should be addressed. FAX: +86-20-39943071. Electronic mail: chenzg@mail.sysu.edu.cn

embryonic zebrafish is a desirable alternative as a whole-organism model to screen new compounds or to evaluate clinical drugs, regardless of the specific therapeutical targets.

Unfortunately, several concerns with static exposure to zebrafish eggs limit their promise for application in toxic and teratogenic evaluation. One typical problem is the irreversibly gradual reduction of the exposed solution because of evaporation and nonselective adsorption, which lead to uncontrolled changes of concentration and pH of the original solution. To address this problem, a modified 24-well microplate based flow-through system has been developed that can alleviate but do not totally eliminate the issue.<sup>6</sup> Regrettably, this method brings another obstacle that it would deplete large volumes of solutions, which is neither environment friendly nor inexpensive, especially for the toxic or rare test substances. In addition, precise manipulation and serial dilution of chemicals are technically infeasible and labor-intensive to microwell-based analysis in common laboratories. Therefore, there is a great need to establish a facile and multifunctionally integrated platform for pharmaceutical toxicological evaluation using a whole-organism model. The platform cannot only reduce the undesirable surface fouling, slow down or stop the evaporation, but form and guide small volumes of stimuli on demand.

Microfluidic technology has a great potential to meet the requirements. Currently, microfluidics have proven to be a highly effective way to connect life science with the micro- and nanoworld due mainly to the flexibility of microchannel networks and the integration of varied functional elements.<sup>7,8</sup> To date, a number of biomedical application, such as cell-based investigation, in particular, cell cultivation and proliferation has been shown to great success relied on microfluidic chip.<sup>9,10</sup> Apart from cells,<sup>11–13</sup> embryos,<sup>14–18</sup> nematodes,<sup>19–22</sup> and tissues,<sup>23,24</sup> all have realized on-chip cultivation or manipulation. However, the microscale channels fail to easily handle the multicellular organism of large size, such as zebrafish embryos, which might obscure their promise of application in compound-related toxicity and teratogenicity assay. Recently, there has been a trend for zebrafish-related study turning to lab-on-a-chip, such as high-efficient embryonic microinjection,<sup>25</sup> high-throughput embryonic droplets generation,<sup>26</sup> and digital transportation of droplet encapsulated embryo,<sup>27</sup> ranging from dynamic manipulation to static stimulation by electroporation<sup>28</sup> and microfluids.<sup>29</sup> However, the microscale droplet is ill suited for long-time culture of embryos, particularly in small-size segments,<sup>26</sup> and the autocrine or paracrine may affect their normal development. Although the on-chip research for zebrafish (embryos) have been successfully performed, their significant application in drug discovery and toxic assessment are still limited, and the corresponding technical challenges also exist.

In this work, we describe a phenotype-based whole-organism model to evaluate the developmental toxicity and teratogenicity of drugs induced zebrafish embryos using an integrated array microfluidic device. By incorporating a concentration gradient generator and arrayed embryonic culture chambers into a single three-layer microdevice, the gradient and continuous exposure for fish eggs can be realized. This microfluidic system not only continually delivers test substances but also allows sufficient flowing streams to compensate for the lose of evaporation and non-specific adsorption and to properly remove the harmful excretive waste and metabolite within long periods. Also, the reusable glass chip with natural hydrophilicity can effectively reduce the non-selective adsorption and eliminate evaporation in microchannel area. The method presented here can bridge the gap between animal model and the complex microscale stimulation, which permits a whole-organism-level way to assess the clinically available drugs by scoring teratogenic severity. The simple characterization provides a better understanding how the test substances induce the developmental malformations by monitoring the sensitive tissues in a continuous or a stage-specific exposure manner. The integrated microfluidic system should be useful in phenotype-based pharmaceutical evaluation via easy operation, thus holds great promise in high-throughput toxicant and drug screening.

## II. EXPERIMENT

### A. Design and fabrication of microfluidic device

The microfluidic chip consisted of a slide of top glass plate etched with a concentration gradient generator (CGG) and a middle plate containing an array of independent embryonic

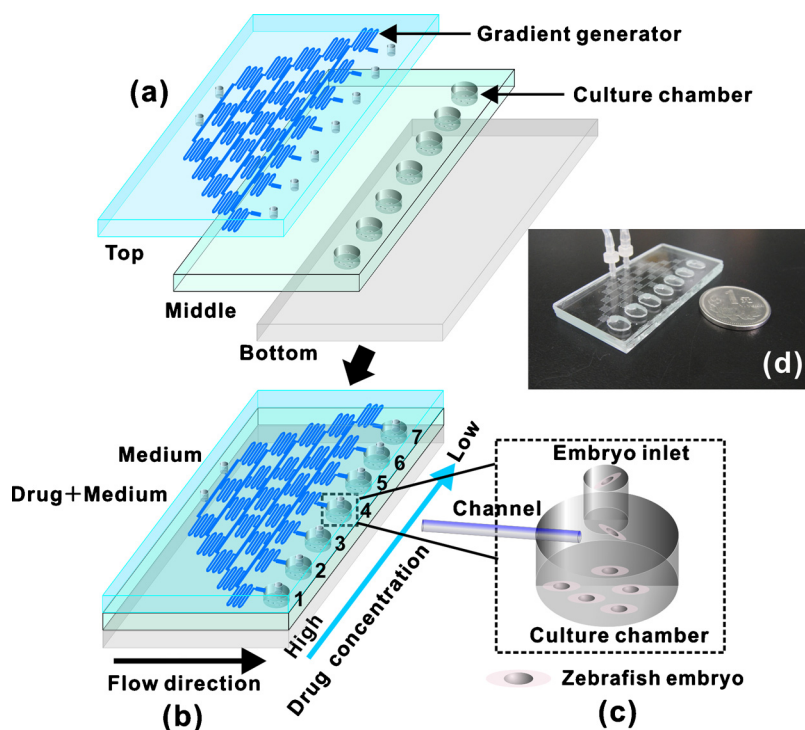


FIG. 1. Schematic of an integrated microfluidic chip for embryonic zebrafish assay. (a) A three-layer microfluidic chip: a top plate with a concentration gradient generator (CGG) and embryonic inlet array, a middle plate with a set of independent array chambers (1–7) for embryo culturing, and a bottom layer. (b) The assembled microfluidic device, with two inlets of solution (medium and drug+medium), used to generate drug gradients, in order, from chambers 1 (high) to 7 (low), and then exposure to the embryos trapped in the culture rooms. (c) Magnified section of a single chamber structure including an embryo inlet from the device upper layer, and a culture compartment containing several embryos, sandwiched between inlet and bottom plate, with connection to a flowing microchannel. (d) A photograph of the fabricated microfluidic chip.

culturing chambers, as well as a cover plate [Fig. 1(a)]. The design of the microfluidic networks was relied mainly on the previous work described by Jeon *et al.*<sup>30</sup> and Liu *et al.*<sup>31</sup> The microscale network on the top plate comprised an upstream gradient generator and a series of downstream inlets for embryonic introduction and waste discharge, which is functionally similar to the central outlet in the multi-pyramidal structure presented by Lin's group.<sup>32</sup> After loading the medium with and without pharmaceuticals into the device by syringe pump (LSP10-1B, LongerPump, Baoding, China), the streams were driven to split, combine, mix, and that repeated several times, which resulted in seven gradient concentrations perpendicular to the flowing direction. The resulting gradient solutions were then guided to stimulate the embryos trapped in well-defined chambers.

In the fabrication processes, the treated three-layer glass slides were aligned and then irreversibly bonded by high temperature (550 °C). Prior to bonding, the microchannel networks were patterned onto a glass plate by standard photolithographic and wet chemical etching techniques.<sup>33</sup> Briefly, a negative film mask with microchannel design was prepared and then the channel patterns were transferred onto a  $6.3 \times 6.3$  cm<sup>2</sup> glass plate (Shaoguang Microelectronics Co., Changsha, China) with photoresist coating by UV exposure. After treatment with developer, the desired image was developed. The untreated photoresist was solidated and the appeared chromium layer was removed. Then the naked micropatterns on the surface of glass slide were etched in dilute HF+NH<sub>4</sub>F bath. The top slide contained the CGG microchannels (120 μm wide and 30 μm deep), connective channels (300 μm wide and 30 μm deep) and seven embryo inlets (about 1.3 mm in diameter) drilled with a diamond drill bit at the channel terminals. The dimension of the sandwiched culture chambers was about 4.0 mm in diameter and 1.70 mm in depth (thickness of glass plate), drilled with a large size emery drill-bit at the previously printed pattern. Thus, the

simple and compact embryonic trapping room was fabricated to provide suitable culturing microenvironments for the eggs. Prior to the following application, the device was cleaned and sterilized.

## B. Organism

The wild-type zebrafish (provided by School of Life Sciences, Sun Yat-sen University, China) were housed in a ratio of 2 females to 1 male in stand-alone aquaria with a recirculating system. The fish were kept on a 14 h light/10 h dark cycle and the culture temperature was set at  $26 \pm 1$  °C, as described by Zhou *et al.*<sup>34</sup> Males and females were kept separately until the night before spawning. Then, the eggs of zebrafish were collected in a sedimentation tank by the addition of purpose-built egg traps prior to spawn. The newly fertilized eggs were transferred into Petri dishes filled with embryo medium E3 (5 mM NaCl, 0.17 mM KCl, 0.40 mM CaCl<sub>2</sub>, and 0.16 mM MgSO<sub>4</sub> per 100 ml distilled water). The normally and healthy developed eggs at different developmental stages were then selected under a stereomicroscope (SMZ-T4, Optec, Chongqing, China) for the subsequent microfluidic application.

## C. Embryo trapping, culture, and stimulation on the device

Before embryo loading, the microfluidic device was serially rinsed with 0.1 mol/l HNO<sub>3</sub>, 0.1 mol/l NaOH, distilled water and fish embryo culture media to clean the microchannel surface and to remove bubbles. After being washed with embryonic media, the newly fertilized eggs or stage-dependent embryos were safely transferred into the culture chambers by a modified pipette tip. To facilitate the loading process, each culture compartment should be prefilled with culture medium. As transferred, it could be trapped in the culturing room via gravity-induced gradual subsidence and a single animal could be delivered in each operation. Prior to culturing and treating the embryos, the microchip was leaned over the Petri dish margin at an angle approximately 20° to facilitate the waste discharge and maintain adequate oxygen for embryonic development. In the experiment, embryo culture medium containing 10 or 100 μg/ml doxorubicin (DOX, Sigma Chemicals, St. Louis, MO) and blank culture medium were introduced to the two inlets, respectively. The flowing stream was driven by the syringe pump with positive pressure at a flow rate of 4 μl/min and the leaned microchip was kept at 26 °C to benefit the embryonic development. The embryos of 1, 4, 12, and 24 hpf (hours postfertilization) were selected and continuously exposed to the same concentration of stimuli (100 μg/ml) for 23, 68, 24, and 24 h, respectively. In addition, the eggs of 1 hpf were also stimulated by 10 μg/ml DOX until 24 hpf. Moreover, embryos at 4 hpf were exposed to other drugs such as 5-fluorouracil (5-FU, Sigma Chemicals, St. Louis, MO), cisplatin (DDP, Sigma Chemicals, St. Louis, MO) and Vitamin C (Vit C, Sigma Chemicals, St. Louis, MO) with seven concentrations ranging from 0 to 100 μg/ml based on the previously presented CGG networks, up to 72 hpf. After stimulation, the test chemicals were removed and left the embryos for further observation.

## D. Assessment of toxicity and teratogenicity

Several toxic and teratogenic events were evaluated, including developmental toxicity of stage-specific stimulation and continuous stimulation, and typical teratogenic effects after stimulation from 4 to 72 hpf, in embryonic zebrafish by an integrated microfluidic device. The micro-scale networks provided gradient DOX solutions to stimulate the eggs and generate toxic and teratogenic impairments. Based on well-documented morphology at a variety of developmental stages,<sup>35</sup> a physiologically precise evaluation regarding the toxicity and teratogenicity on the embryos can be carried out by morphological analysis. At different growth stages, it was necessary to record varied representative signs such as heart rate, pericardium and yolk shape, spontaneous motion or body twisting, number of somites, the development of eyes, notochord and body shape, tail fin size, pigmentation, and so on. The toxic assessments were mainly characterized with developmental arrest, spontaneous movements, and heart rates. To get physiologically real cardiac activity, heart rate of the control and DOX-treated embryo was directly counted by the naked eye

under a stereomicroscope for 20 s and the data were multiplied by 3 (times/min). The spontaneous movement was also calculated in the same manner. Then, we made a detailed estimate relied on the records and scored them by the malformed severities. The scoring system mainly aimed at body teratogenic shape, notochord, and tail fin morphology in this work. The toxicities of other drugs were predicted upon the DOX-induced toxic severity. For instance, in a numerical score system, the normally structured embryo in controls was allocated a score of 0 like No.7 and that the variation within the normal range was signified with a score of 1 like No.6 [Fig. 4(a) and 4(c)]. Scores of 2 or above manifested deformation with increasing severity (2=mild malformation like No.5; 3=clear malformation like Nos. 3 and 4; 4=severe malformation like No. 2; 5=dead like No. 1).

### E. Image analysis

For a clear verification of the toxic impact of the used testing substances on the embryonic development, several end points were documented by employing an inverse optical microscope (4×, 10× objective, BDS200, Optec, Chongqing, China) with a digital camera (DM200). We mainly selected heart rate, body twisting, pigmentation, tail detachment, development of eyes, segmentation, and teratogenicity as evaluating end points. Differences to the normal development were measured by these end points. The morphological and developmental variations were recorded and examined at specific developmental stages (initial stage at 1 or 4 hpf, and then 12, 24, 36, 48 hpf, as well as that at more than 48 hpf observed once every 12 h until 120 hpf) for the individual egg trapped in the culture room. The recorded photographs were analyzed using OPTPRO software by its measuring and photoprocessing function. To get comprehensive and detailed data of the deformations caused by the chemical stimuli, 10× objective was used to obtain the enlarged target feature.

## III. RESULTS AND DISCUSSION

### A. Design and characterization of the integrated microdevice

A microfluidic chip was fabricated using three layers of glass plate by integrating an array of embryo trapping chambers with a concentration gradient generator. It was observed that the embryos, when manipulated by a modified pipette tip and transferred to culture chambers, could grow normally without obvious lesion (supplementary material Fig. S11).<sup>36</sup> As transferred to the open-access embryonic inlet, the embryo could spontaneously precipitate on the chamber bottom for trapping by its nonviscous sedimentation [Fig. 1(c)]. This property contributed to the stable position of embryos under the flowing system, and enabled the microfluidic chip that applied in fish embryo-associated assay to be used repeatedly comparable to the microdevice for cell-based assay.<sup>37</sup> In the tests, we placed the microfluidic device at an angle of about 20° to horizontal level to facilitate the withdrawal of waste without additional use of tubes, and the open culture chamber can still maintain the normoxia development for embryos that was particularly important for larvae.<sup>38</sup> The open surface design together with gradient soluble molecules were not only well-suited for cell-based research,<sup>39</sup> but benefited zebrafish embryo-related investigation that even did not need a CO<sub>2</sub> culture incubator. But the irreversible evaporation was still an issue. The problem can be attenuated by slightly increasing the injection flow velocity (3–5 μl/min) to counteract the liquids loss. Furthermore, between the embryonic inlet and culture chamber, a segment of widened microchannel (300 μm wide) was designed to slow down the flow rate for decreasing the harmful fluidic shear stress [Fig. 2(a)], which would be more serious if the microchannel was etched at bottom of the middle plate. In this experiment, in order to facilitate the imaging, a flow velocity as high as 50 μl/min was used to remove the remanent drugs or labels. The rapid elution (within 96 s) process was indirectly characterized by diluted methylene solution [Fig. 2(b)]. The high flow rate may move, or even impair the embryos as the widened channels were fabricated at surface of the chamber bottom.

Another important aspect of this microfluidic device, concentration gradient generator (CGG), has attracted more and more attention recently.<sup>39–44</sup> We presented a gradient network with seven

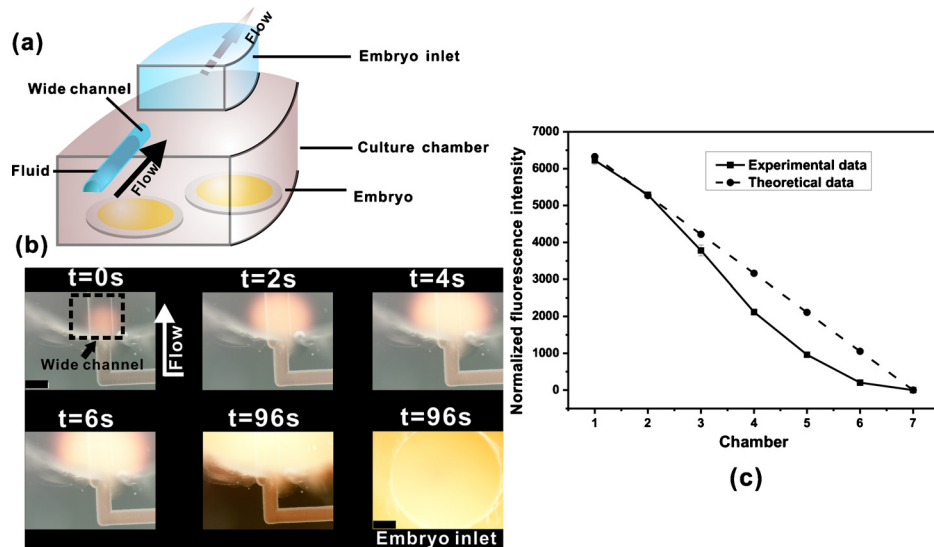


FIG. 2. (a) A cross-section view of fluid direction in the chamber (arrow). (b) The microphotographs of modeling perfusion process in embryo culturing room by methylene blue. The chamber was filled within 96 s under a eluting rate of  $50 \mu\text{l}/\text{min}$  with weak shear stress by wide microchannel (black rectangle). The scale bar is  $300 \mu\text{m}$ . (c) The fluorescent intensities of  $10 \mu\text{M}$  sodium fluorescein were quantified ( $n=3$ ), the background fluorescence was subtracted, and a comparison was made between the experimental data and theoretical data.

branches of concentration at a spatial resolution based on previously employed principle of laminar flow in microchannels,<sup>30</sup> and  $10 \mu\text{mol}/\text{l}$  sodium fluorescein was applied to quantify the resultant concentrations in the culture chambers. Although the fluorescent probes have a slightly higher diffusion coefficient than the test substances due in part to varying molecular weight between them (DOX,  $580.0 \text{ g}/\text{mol}$ ; sodium fluorescein,  $376.3 \text{ g}/\text{mol}$ ), the long serpentine channel would allow effective mixing for input solutions. Also the enough mixing can be achieved by modulating the injection flow rates to prolong the diffusion time. Furthermore, mathematical prediction was applied to estimate the concentration profile of the drugs in the culture chamber and make a comparison between the theoretical data and the experimental results. Equation (1) is an efficient mathematical formula, which is derived from the significant equation described by Jeon *et al.*,<sup>30</sup> to predict the theoretical value of  $C(i,N)$ .<sup>42</sup>

$$C(i,N) = \frac{(N-i)C_1 + iC_2}{N}, \quad (1)$$

where  $C(i,N)$  signifies concentration at the end of serpentine channel,  $N$  represents the number of order (from the top) of the microfluidic gradient microchannels ( $N=1,2,3,4,5,6$ ), and  $i$  means the number of order (from left) of the branch point ( $i=0,1,2,3,4,5,6$ ). Thus, when  $C_1$  is  $100 \mu\text{g}/\text{ml}$  and  $C_2$  is  $0 \mu\text{g}/\text{ml}$ , seven culture chambers (Nos. 1–7) are expected to have No. 1,  $C(0,6)$ ,  $100 \mu\text{g}/\text{ml}$ ; No. 2,  $C(1,6)$ ,  $83.3 \mu\text{g}/\text{ml}$ ; No. 3,  $C(2,6)$ ,  $66.7 \mu\text{g}/\text{ml}$ ; No. 4,  $C(3,6)$ ,  $50 \mu\text{g}/\text{ml}$ ; No. 5,  $C(4,6)$ ,  $33.3 \mu\text{g}/\text{ml}$ ; No. 6,  $C(5,6)$ ,  $16.7 \mu\text{g}/\text{ml}$ ; No. 7,  $C(6,6)$ ,  $0 \mu\text{g}/\text{ml}$ . From the results of concentration profile as shown in Fig. 2(c), it was found that the experimental data were correlated well with the theoretical prediction,<sup>30</sup> and the central parts of channels with more errors presumably ascribed to the hydraulic defocusing at the merged points.<sup>42</sup> By comparing with previous similar works,<sup>37,42</sup> the data obtained here matched them well.

## B. On-chip embryonic development

Because of the special features of zebrafish embryo such as nonviscous sedimentation and larger size than cell, we specifically fabricated a facile and flexible two-layer pore structure [Figs. 1(c) and 2(a)], and the bottom large well was utilized for trapping more than one embryo (3 each

well), meanwhile offering broad space for their normal growth.<sup>26</sup> When we connected the embryo inlet with small-size Teflon tube (I.D. 500  $\mu\text{m}$ ) to allow outflow of waste, an obvious developmental arrest occurred at 24 hpf and the results became worse as the time passed. At approximately 48 hpf, it was found that the incompletely developed eggs could not recover from culture rooms after removing the tubes (supplementary material Fig. SI2).<sup>36</sup> This finding was consistent with the previous reports described by Mendelsohn *et al.*<sup>45</sup> and Padilla *et al.*<sup>46</sup> The observations demonstrated that embryonic zebrafish can still survive after oxygen deprivation (anoxia, 0% O<sub>2</sub>), and enter a state of suspended animation where the cell division and other developmentally related progression inhibited or even ceased. Besides, 52 hpf was identified as the lethal point regardless of the anoxia- and normoxia-exposed time.<sup>45</sup> Therefore, the open surface design was crucial for maintaining the normal development for the vertebrate species. Moreover, the fluidic shear stress was another important factor for their normal growth. Recently, Giridharan *et al.* reported that the fluid shear stress was significant (10 dynes/cm<sup>2</sup>) at the height of 200  $\mu\text{m}$  when the well was 250  $\mu\text{m}$  in depth.<sup>47</sup> However, the exposed shear stress, at the same height in the well of 2 mm in depth, was about 0, regardless of whether the fluid shear stress on the order was more than 10 dynes/cm<sup>2</sup> or not. In this work, the positioned spherical embryo was attached on the bottom surface of culture chamber with a height approximately 500  $\mu\text{m}$ , whereas the well was as high as 1700  $\mu\text{m}$ . Additionally, the flow rate (24 mm/s) presented in the above mentioned model was much higher than that (4  $\mu\text{l}/\text{min}$ ) used in our tests. Thus, the effect of the fluid shear stress in the test was negligible. To investigate the effect of flow rates on the trapped embryos, the high flow velocity of medium injection above 100  $\mu\text{l}/\text{min}$  had been employed but did not exert negative impact on the normal development of the embryos even at the early stage (1 hpf) (supplementary material Fig. SI3),<sup>36</sup> a stage more sensitive to the exogenous stimulation.<sup>48</sup>

### C. Developmental toxicity and teratogenicity of DOX on zebrafish embryos

As a whole-organism model, zebrafish embryo was proved to be effective for phenotype-based screening of antiproliferation metallodrugs.<sup>4</sup> DOX is one of the most effective chemotherapeutic agents, but its wide use was seriously limited by the chronically clinical side effects such as irreversible off-target cellular antiproliferation and cardiomyopathy.<sup>49</sup> In this work, DOX was applied as a model drug to stimulate zebrafish embryos by its antiproliferating activity, cardiotoxicity, and other teratological effects. The acute embryotoxicity of DOX exhibited an obvious time- and dose-dependent toxicity and the LD<sub>50</sub> of DOX to the embryo was 91.7  $\mu\text{g}/\text{ml}$  in microwell (supplementary material Fig. SI4).<sup>36</sup> To establish a zebrafish-based evaluation model for predicting the potential toxicity of clinical agents using an integrated microfluidic device, we particularly examine the developmental inhibition and teratogenicity of DOX on zebrafish embryo.

#### 1. Developmental stage-specific stimulation for embryonic developmental toxicity

During the periods of rapid embryogenesis, a variety of representative developmental stages have been defined, such as zygotic cell, cleavage, blastula, gastrula, segmentation, pharyngula, and hatching period, to allow subsequent incorporation of new observations and details, and to facilitate the investigation related to embryonic development.<sup>35</sup> For 1h old embryos, a low concentration (10  $\mu\text{g}/\text{ml}$ ) has been used to stimulate the arrayed eggs from 1 hpf (cleavage period) to 24 hpf (segmentation period) because DOX up to 100  $\mu\text{g}/\text{ml}$  would result in high lethality (supplementary material Fig. SI4).<sup>36</sup> As shown in the Fig. 3(a) (24 hpf), the results exhibited developmental inhibition, in particular, for the highest concentration drug-treated embryo (trapped in No. 1 chamber) which stopped at approximately 10 hpf without further growing. Theoretically, the heartbeat, early pigmentation and tail extension would occur at the 24 hpf.<sup>35</sup> However, it was observed that only the No. 7 individual was pigmented mildly in the skin epithelium and accompanied with feeble heartbeat in rhythm. While removing the test compounds from exposure at the time that could significantly increase the hatching success by transferring them into the multiwell plate filled with culture medium [Fig. 3(a), 60 hpf]. Obviously, it was found that the No. 1 embryo was irreversibly affected, while the others seemed to recover from compounds-induced damage

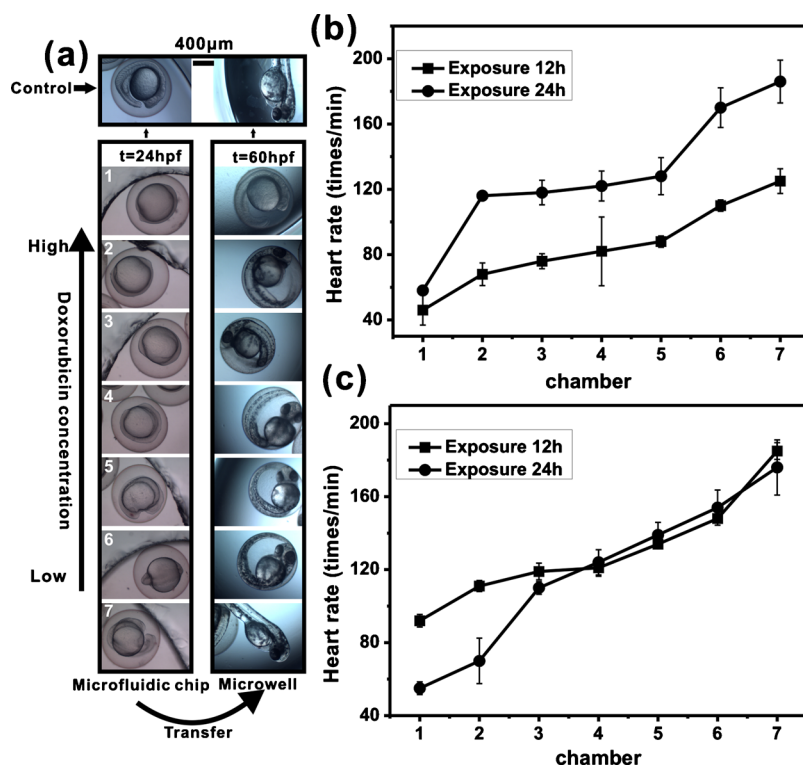


FIG. 3. Zebrafish embryos of different developmental ages used to test the toxic effects of gradient doxorubicin (DOX). (a) Embryos of 1 hpf (hours post-fertilization) were exposed to 0–10  $\mu\text{g}/\text{ml}$  DOX until 24 hpf and then transferred into microwells to observe the developmental toxicity. [(b) and (c)] Embryos of 12 hpf and 24 hpf were continuously exposed to 0–100  $\mu\text{g}/\text{ml}$  DOX until 36 hpf and 48 hpf, respectively. The cardiotoxic effects were characterized by heart rate per 12 h exposure ( $n=3$ ).

and successfully hatched. Several described acute side effects on humans resulted from DOX were also reversible.<sup>50</sup> Additionally, we observed apparent developmental suspension of embryos in the microplates since exposure to 10  $\mu\text{g}/\text{ml}$  doxorubicin from 1 hpf to 24 hpf, and 10% mortality appeared at 72 hpf under continuous incubation (supplementary material Fig. SI4).<sup>36</sup> The results demonstrated that the low concentration test substances can negatively affect the development of zebrafish embryo at early pre-hatching stage (1–24 hpf), but the influence seem to be temporary and that might be gradually resumed after removing exposure. In addition, both 12 hpf and 24 hpf old embryos were exposed to DOX (injected at 100  $\mu\text{g}/\text{ml}$ ) up to 36 hpf and 48 hpf, respectively, and then transferred into breeding microwells to observe the toxic effects and teratogenic appearances when hatching. It was found that there was a negative correlation between the heart rate and the exposed concentration for both groups [Figs. 3(b) and 3(c)], and the developmental process for them was showed in supplementary material (Figs. SI5 and SI6).<sup>36</sup>

## 2. Continuous stimulation for embryonic developmental toxicity

To obtain better understanding of DOX-induced potential damage on the zebrafish embryos, a strategy of long time and consistent exposure was performed. The continuous stimulation was used spanning a time period from 4 hpf (blastula period) to 72 hpf (hatching period). Up to 24 hpf, morphological assay exhibited that tail detachment, and clear segmentation all occurred on the embryos, but mild pigmentation, weak heartbeat, as well as blood circulation only appeared on the eggs in the chambers 5–7 [low concentration zone, Fig. 4(a)(A)]. Moreover, a typical developmental property aroused at this stage was the spontaneous movements, which was examined as an indicator for embryonic development. Obviously, the rate of spontaneous contractions of each embryo responded with a concentration-dependent increase and the embryo was insensitive to the



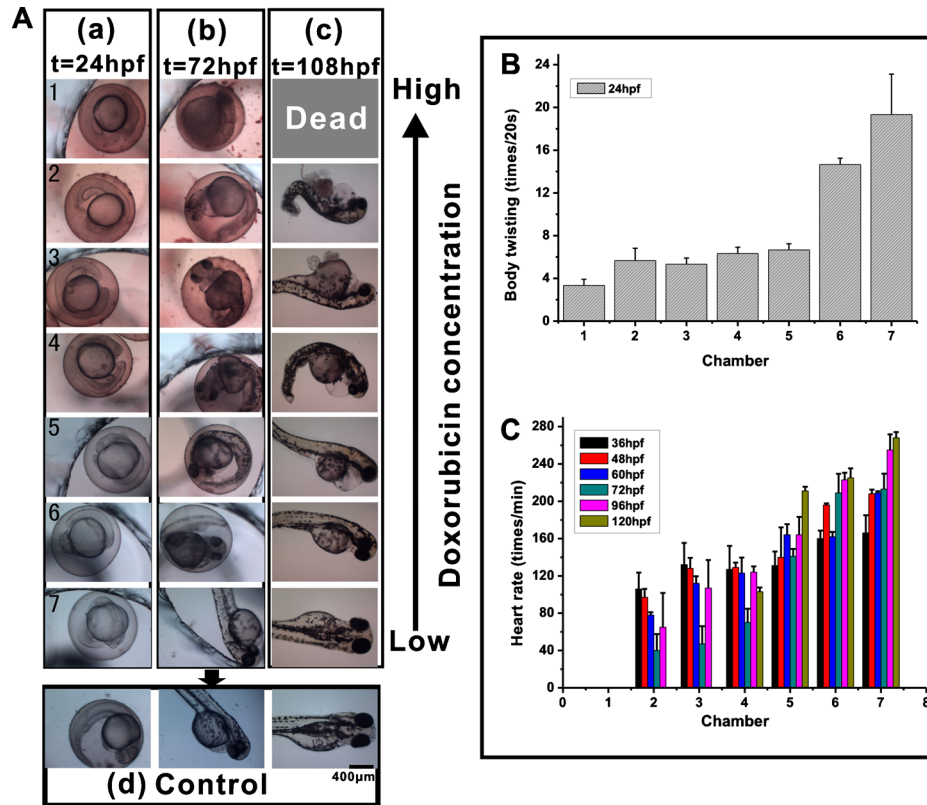


FIG. 4. The toxicity of continual stimulation by DOX gradients (0–100  $\mu\text{g}/\text{ml}$ ) on the zebrafish embryos of 4 hpf. (a) Representative images of the exposed embryos at 24 hpf (A) and 72 hpf (B), and then stop stimulation, after removing drug solutions, the trapped embryos keep developing until 108 hpf in culture chamber (C). All embryos and larvae were imaged by inverse light microscopy at a magnification of  $\times 40$ . (b) At 24 hpf, embryos were developed to twist their bodies, the twisting frequency exhibits a dose-dependent decrease ( $n=3$ ). (c) The heart rates of embryos from 36 to 120 hpf (including consistent drug exposure to 72 hpf and then suspending exposure to 120 hpf) demonstrated a dose-dependent decrease but irregular change for time dependence ( $n=3$ ).

DOX when the exposure concentration was lower than 16  $\mu\text{g}/\text{ml}$  approximately [Fig. 4(b)]. However, our observed spontaneous coiling rates in zebrafish embryos were not the same as the previous report, where a phenomenon was that the spontaneous and alternating contractions of the trunk initiated at 17 hpf with a frequency of 0.57 Hz, reached the peak at 19 hpf with 0.98 Hz, and then gradually decreased to less than 0.1 Hz by 27 hpf.<sup>51</sup> Based on that, the spontaneously contracting frequency observed in our research achieved the peak at 24 hpf. The delay in spontaneous activity presumably resulted from the overall slowing or inhibition of growth in embryos raised at lower temperature.<sup>35</sup> Then, it was found that the embryonic diapause occurred at 36 hpf in chamber 1 and the embryo died at 72 hpf approximately [Fig. 4(a)(b)]. Similarly, the eggs in chamber 2 also showed diapause at 48 hpf and that emerged at 60 hpf in chambers 3–5, as well as clear developmental retard for the embryos in chamber 6 at 72 hpf [Fig. 4(a)(b)]. When exposure time was up to 72 hpf, we removed the test substances and returned the treated eggs to drug-free culture medium for subsequent observation. At approximately 96 hpf, the damaged embryos were dechorinated manually to facilitate the teratogenic examination, because of incapability of breaking through the chorion spontaneously. As shown in the Fig. 4(a)(c), the toxic and teratogenic severity were typically increased in concentration-dependent for the zebrafish embryos exposed to the gradient DOX. Furthermore, heart rate, as another vital evaluating index, allowed varied end points to be recorded to estimate the developmental toxicity. The results exhibited a marked concentration-responsive decrease for the heartbeat rates [Fig. 4(c)]. Up to 120 hpf, the larvae in chamber 2 and 3 also died due to the irreversibly embryonic toxicity albeit temporal alleviation

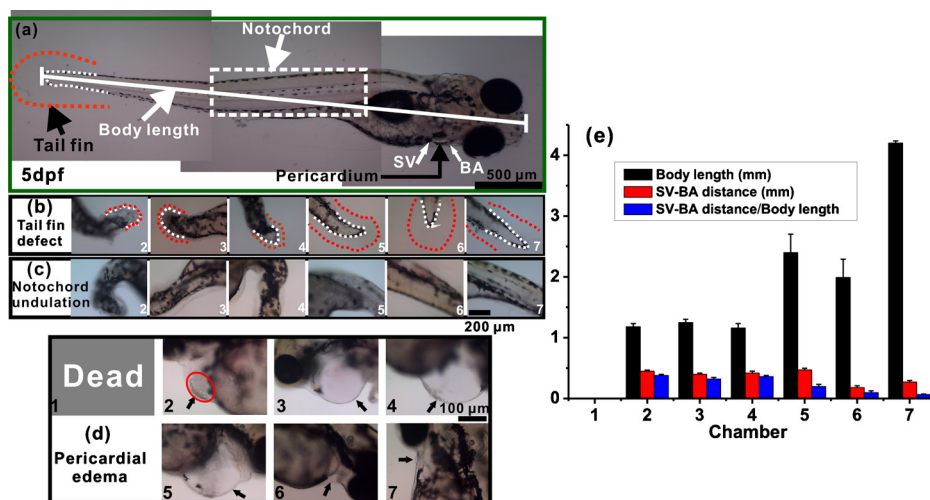


FIG. 5. The teratological effects of DOX-exposed zebrafish embryos. (a) A side view of a normal larval fish with 5 dpf (days postfertilization), the typical sensitive tissues or organs including pericardium, tail fin (area between the red and white dot line), notochord (white rectangle), sinus venosus (SV), and bulbus arteriosus (BA). Body length signified by white oblique line. Tail fin defects (b) and notochord undulation (c) for array larvae. (d) Pericardial edema (black arrow) for array larvae exposed to gradient DOX from 4 to 72 hpf. No. 1 died and No. 2 with obvious red cells accumulation (red ellipse). (e) Body length, distance between the SV and BA (SV-BA distance), and SV-BA distance/body length of the exposed embryos were plotted and SV-BA distance/body length were concentration-dependent ( $n=3$ ).

(from 72 to 96 hpf) occurred for them. Additionally, during the entire observation periods, the embryos in chambers 2–5 reached the minimal heartbeat at 72 hpf, which showed that the continuous exposure to doxorubicin above approximately  $30 \mu\text{g/ml}$  could cause severe cardiotoxicity for 4 hpf embryos.

### 3. Teratological effects on embryonic development

Morphological analysis uncovered a large suite of malformations including pericardial edema, undulated notochord, reduction or absence of tail fin, crooked trunk, less melanin pigmentation, fuzzy somites, and other defects [a normally developed body structure was exhibited in Fig. 5(a)]. However, the most sensitive tissue was proved to be pericardium, following by tail fin and notochord after exposure to DOX. Pericardial edema, as an important signal in embryonic developmental toxicity triggered by chemicals, appeared such prominently in DOX-treated embryos [Fig. 5(b)]. The impairment began to be remarkable more or less at 36 hpf, in particular, for the embryo in chamber 4 (supplementary material Fig. S17).<sup>36</sup> But it was not apparent in both the higher concentration exposed eggs and the lower ones presumably due to the developmental retard and insufficient toxicity, respectively. The impairing severity was clearly identified as a time- and concentration-dependent increase at 108 hpf [Fig. 5(b)]. In addition, DOX could destroy myocardium and lead to irregular heart rate or bradycardia, and even heart failure during the period of cardiogenesis.<sup>50</sup> The findings were indirectly exhibited in Fig. 4(C). Besides that, red cells accumulated on the surface of the swollen pericardium, particularly on No. 2 embryo [Fig. 5(b)].

Instead, tail fin generated a series of malformations involving reduction or absence of fin after DOX treatment. The tail fin defects showed a concentration-responsive increase and might be categorized by scoring system to predict the toxic potential of the compounds that was specifically sensitive to tail fin or tail [Fig. 5(c)], such as antitumor metallodrugs and ruthenium (Ru) derivatives, presumably due to the Ru-induced apoptosis of proliferating fin mesenchymal cells.<sup>4</sup>

With respect to another sensitive tissue to DOX, notochord was characterized with typical abnormality like undulated notochord or crooked trunk. The malformed severities were presented with a concentration-dependent response to the drug [Fig. 5(d)]. Similar notochord deformity resulted from cartap exposure was reported by Zhou *et al.*<sup>54</sup> They found that a temporal exposure

(6–8 h) can cause obvious undulated notochord phenotype during a development window from 6 to 32 hpf, and the eggs in stage of 6–24 hpf were more sensitive to cartap as compared to those in stage of 24–32 hpf, which was consistent with the study in DOX-induced toxicity assay to 12 hpf embryos. The possible mechanism for DOX-induced notochord malformation may be the impairment on sheath matrix enzyme lysyl oxidase. The notochord-specific chemicals such as cartap were also suited to be evaluated by scoring method.

To better examine the heart malformation in the DOX-exposed embryonic zebrafish, the distance between the sinus venosus (SV) and bulbus arteriosus (BA) was measured to provide an index of the cardiac looping, which transformed into two distinctive heart chambers (atrium and ventricle).<sup>52,53</sup> As shown in Fig. 5(e), clear difference occurred in this distance between the treated embryos and the control (No. 7). It demonstrated a gradual reduction in the ratio of SV-BA distance to body length as the exposed concentration decreased. The data aided to identify the negative effect of DOX on the cardiogenesis in zebrafish embryos.

#### D. Prediction of the potential toxicity of drugs

To gain a better understanding of the embryotoxicity and teratogenicity of the clinical or preclinical available drugs, an evaluating system based on teratogenic severity by scoring needs to be established. A similar method has been described by Brannen *et al.*<sup>54</sup> The presented estimations were determined relied heavily on the presence or absence of defects and the identification of a concentration-responsive increase in those abnormalities above background level. Thus, a morphological score system might be used as an assessing method to predict *in vivo* toxic and teratogenic potentials of drugs. Subsequently, we carried out the toxic assay regarding 5-fluorouracil (5-FU), cisplatin (DDP), and ascorbic acid (Vit C) on the 4 hpf embryo of zebrafish via the assessing model for their similar action mechanism using the same device. The results, at a variety of toxic end points, were showed in Table I. It was found that ADM and DDP had comparative toxicity and teratogenicity by exposing to 4 hpf zebrafish embryo at the same dosage level. This result may originate from their similar pharmacological mechanism (impairing DNA structure). Compared to these two agents, the embryonic toxicity of 5-FU was halved under the same conditions. When the embryos were treated by Vitamin C (0~100  $\mu\text{g}/\text{ml}$ ), there was no apparent damage to them. In this study, notochord, tail, and fin were identified as the most sensitive tissues to the testing compounds. In addition, pigmentation and heart rate, as critical and accessible physiological index, also had important implications. Hence, by ranking these susceptible tissues and life indicators in terms of the severity of teratogenicity and toxicity, we can obtain a quantitative assessment and prediction for more drugs by scoring based on a fundamental standard. The purpose of this work was to validate the feasibility of developing a microfluidics-based whole-animal model for evaluating chemical-induced toxic and teratogenic effects on embryonic zebrafish. Therefore, the score protocols had not been used to predict and assess other more compounds. This issue can be addressed in the near future by increasing the array units and fabricating more well-defined culture structures.

#### IV. CONCLUSIONS

An efficient integrated microfluidic array system has been developed to evaluate the dynamic developmental toxicity and teratogenicity for clinical drugs on the zebrafish embryos. This microfluidic device offers an opportunity to integrate the entire operations, including gradient concentration generation, egg positioning, egg culture, drug stimulation, real-time monitoring, and seamless combination of drug gradient with arrayed embryonic culture chambers. Such a microsystem was used to assess and predict the potential toxicity of the antiproliferating drugs (DOX, 5-FU, DDP) on zebrafish eggs at a variety of different developmental stages. By real-time monitoring at significant physiologically related developmental stage, the presence, absence, or reduction of typical developmental appearance can be well documented for subsequent scoring assay. Therefore, we can establish a sensitive whole-animal model to evaluate the toxicity of target-specific chemical agents or drugs via scoring system based on the abnormality severity. But it needs

TABLE I. Parallel toxic evaluation in zebrafish embryo assay. ADM: adriamycin or doxorubicin; 5-FU: 5-fluorouracil; DDP: cisplatin; Vit C: Vitamin C; n 1–7 refer to the corresponding culture chamber numbers 1–7.

| Compound | Pharmacological target      | Classification | Concentration tested ( $\mu\text{g}/\text{ml}$ ) | Morphological end points and scoring assessments |     |     |     |     |     |     |     |
|----------|-----------------------------|----------------|--------------------------------------------------|--------------------------------------------------|-----|-----|-----|-----|-----|-----|-----|
|          |                             |                |                                                  | n                                                | 1   | 2   | 3   | 4   | 5   | 6   | 7   |
| ADM      | Impairing DNA structure     | Teratogen      | 0–100                                            | a                                                | 5   | 4   | 3   | 3   | 2   | 1   | 0   |
|          |                             |                |                                                  | b                                                | 5   | 3   | 4   | 4   | 2   | 1   | 0   |
|          |                             |                |                                                  | c                                                | 5   | 3   | 4   | 4   | 2   | 1   | 0   |
|          |                             |                |                                                  | d                                                | 5   | 3   | 4   | 4   | 2   | 1   | 0   |
|          |                             |                |                                                  | e                                                | A   | N   | N   | N   | A   | N   | N   |
|          |                             |                |                                                  | f                                                | A   | A   | A   | A   | A   | N   | N   |
|          |                             |                |                                                  | g                                                | A   | N   | N   | N   | N   | N   | N   |
|          |                             |                |                                                  | h                                                | 0   | 65  | 107 | 124 | 164 | 223 | 255 |
| 5-FU     | Inhibition of DNA synthesis | Teratogen      | 0–100                                            | a                                                | 3   | 3   | 2   | 2   | 1   | 0   | 0   |
|          |                             |                |                                                  | b                                                | 3   | 3   | 2   | 2   | 1   | 0   | 0   |
|          |                             |                |                                                  | c                                                | 2   | 2   | 1   | 1   | 1   | 1   | 0   |
|          |                             |                |                                                  | d                                                | 2   | 2   | 1   | 2   | 1   | 0   | 0   |
|          |                             |                |                                                  | e                                                | N   | N   | N   | N   | N   | N   | N   |
|          |                             |                |                                                  | f                                                | A   | N   | A   | N   | N   | N   | N   |
|          |                             |                |                                                  | g                                                | N   | N   | N   | N   | N   | N   | N   |
|          |                             |                |                                                  | h                                                | 127 | 112 | 161 | 183 | 222 | 237 | 232 |
| DDP      | Impairing DNA structure     | Teratogen      | 0–100                                            | a                                                | 5   | 5   | 4   | 3   | 2   | 1   | 0   |
|          |                             |                |                                                  | b                                                | 5   | 5   | 3   | 3   | 2   | 1   | 0   |
|          |                             |                |                                                  | c                                                | 5   | 5   | 3   | 2   | 3   | 0   | 0   |
|          |                             |                |                                                  | d                                                | 5   | 5   | 3   | 2   | 2   | 0   | 0   |
|          |                             |                |                                                  | e                                                | A   | A   | N   | N   | N   | N   | N   |
|          |                             |                |                                                  | f                                                | A   | A   | N   | A   | N   | N   | N   |
|          |                             |                |                                                  | g                                                | A   | A   | N   | N   | N   | N   | N   |
|          |                             |                |                                                  | h                                                | 0   | 0   | 71  | 102 | 144 | 199 | 232 |
| Vit C    | Combining O                 | Nonteratogen   | 0–100                                            | No obvious impairments                           |     |     |     |     |     |     |     |

<sup>a</sup>Body shape.

<sup>b</sup>Notochord morphology.

<sup>c</sup>Tail morphology.

<sup>d</sup>Fin morphology.

<sup>e</sup>Pigmentation.

<sup>f</sup>Swim bladder.

<sup>g</sup>Cardiovascular function.

<sup>h</sup>Heart rate (a–d: score; e–g: normal or abnormal, N or A; h: heartbeat times/min).

standardization. We believe that the trend of lab-on-a-chip for zebrafish (embryo) will focus on the standardization for groups performing related research, high-throughput manipulation and automation.<sup>55</sup> There would be more significant work on microfluidics-based assay for zebrafish (embryo) or other multicellular organisms (*C. elegans* and *Drosophila melanogaster*) for toxic evaluation or drug screening.

## ACKNOWLEDGMENTS

This work was supported by the National Natural Science Foundation of China (Grant Nos. 20727006, 20875105, and 21075139), Guangdong Provincial Science and Technology Project

(Grant No. 2008A030102009). The authors thank Dr. Wenbin Du of University of Chicago for valuable discussion and revision.

- <sup>1</sup>L. I. Zon and R. T. Peterson, *Nat. Rev. Drug Discovery* **4**, 35 (2005).
- <sup>2</sup>M. Strmac and T. Braunbeck, *Ecotoxicol. Environ. Saf.* **44**, 25 (1999).
- <sup>3</sup>D. S. Peal, R. T. Peterson, and D. Milan, *J. Cardiovasc. Transl. Res.* **3**, 454 (2010).
- <sup>4</sup>Y. H. Wang, C. C. Cheng, W. J. Lee, M. L. Chiou, C. W. Pai, C. C. Wen, W. L. Chen, and Y. H. Chen, *Chem. Biol. Interact.* **182**, 84 (2009).
- <sup>5</sup>L. X. Yang, N. Y. Ho, R. Alshut, J. Legradi, C. Weiss, M. Reischl, R. Mikut, U. Liebel, F. Muller, and U. Strahle, *Reprod. Toxicol.* **28**, 245 (2009).
- <sup>6</sup>E. Lammer, H. G. Kamp, V. Hisgen, M. Koch, D. Reinhard, E. R. Salinas, K. Wendler, S. Zok, and T. Braunbeck, *Toxicol. In Vitro* **23**, 1436 (2009).
- <sup>7</sup>G. B. Salieb-Beugelaar, G. Simone, A. Arora, A. Philippi, and A. Manz, *Anal. Chem.* **82**, 4848 (2010).
- <sup>8</sup>I. F. Cheng, H. C. Chang, D. Hou, and H. C. Chang, *Biomicrofluidics* **1**, 021503 (2007).
- <sup>9</sup>H. Y. Li, J. Friend, L. Yeo, A. Dasvarma, and K. Traianedes, *Biomicrofluidics* **3**, 034102 (2009).
- <sup>10</sup>J. El-Ali, P. K. Sorger, and K. F. Jensen, *Nature (London)* **442**, 403 (2006).
- <sup>11</sup>I. Meyvantsson and D. J. Beebe, *Annu. Rev. Anal. Chem.* **1**, 423 (2008).
- <sup>12</sup>H. X. Song, T. Chen, B. Y. Zhang, Y. F. Ma, and Z. H. Wang, *Biomicrofluidics* **4**, 044104 (2010).
- <sup>13</sup>D. Ma, H. W. Chen, Z. M. Li, and Q. H. He, *Biomicrofluidics* **4**, 044107 (2010).
- <sup>14</sup>C. Han, Q. Zhang, R. Ma, L. Xie, T. Qiu, L. Wang, K. Mitchelson, J. Wang, G. Huang, J. Qiao, and J. Cheng, *Lab Chip* **10**, 2848 (2010).
- <sup>15</sup>S. Raty, E. M. Walters, J. Davis, H. Zeringue, D. J. Beebe, S. L. Rodriguez-Zasa, and M. B. Wheeler, *Lab Chip* **4**, 186 (2004).
- <sup>16</sup>J. Melin, A. Lee, K. Foygel, D. E. Leong, S. R. Quake, and M. W. M. Yao, *Dev. Dyn.* **238**, 950 (2009).
- <sup>17</sup>M. S. Kim, C. Y. Bae, G. Wee, Y. Han, and J. Park, *Electrophoresis* **30**, 3276 (2009).
- <sup>18</sup>E. M. Lucchetta, J. H. Lee, L. A. Fu, N. H. Patel, and R. F. Ismagilov, *Nature (London)* **434**, 1134 (2005).
- <sup>19</sup>W. W. Shi, J. H. Qin, N. N. Ye, and B. C. Lin, *Lab Chip* **8**, 1432 (2008).
- <sup>20</sup>W. W. Shi, H. Wen, Y. Lu, Y. Shi, B. C. Lin, and J. H. Qin, *Lab Chip* **10**, 2855 (2010).
- <sup>21</sup>S. E. Hulme, S. S. Shevkoplyas, J. Apfeld, W. Fontana, and G. M. Whitesides, *Lab Chip* **7**, 1515 (2007).
- <sup>22</sup>K. Chung, M. M. Crane, and H. Lu, *Nat. Methods* **5**, 637 (2008).
- <sup>23</sup>D. Huh, B. D. Matthews, A. Mammoto, M. Montoya-Zavala, H. Y. Hsin, and D. E. Ingber, *Science* **328**, 1662 (2010).
- <sup>24</sup>A. Webster, C. E. Dyer, S. J. Haswell, and J. Greenman, *Anal. Methods* **2**, 1005 (2010).
- <sup>25</sup>A. Noori, P. R. Selvaganapathy, and J. Wilson, *Lab Chip* **9**, 3202 (2009).
- <sup>26</sup>A. Funfak, A. Brosing, M. Brand, and J. M. Kohler, *Lab Chip* **7**, 1132 (2007).
- <sup>27</sup>S. U. Son and R. L. Garrell, *Lab Chip* **9**, 2398 (2009).
- <sup>28</sup>K. S. Huang, Y. C. Lin, K. C. Su, and H. Y. Chen, *Biomed. Microdevices* **9**, 761 (2007).
- <sup>29</sup>Y. C. Shen, D. Li, A. Al-Shoaibi, T. Bersano-Begey, H. Chen, S. Ali, B. Flak, C. Perrin, M. Winslow, H. Shah, P. Ramamurthy, R. H. Schmedden, S. Takayama, and K. F. Barald, *Zebrafish* **6**, 201 (2009).
- <sup>30</sup>N. L. Jeon, S. Dertinger, D. T. Chiu, I. S. Choi, A. D. Stroock, and G. M. Whitesides, *Langmuir* **16**, 8311 (2000).
- <sup>31</sup>D. Y. Liu, L. J. Wang, R. T. Zhong, B. W. Li, N. N. Ye, X. J. Liu, and B. C. Lin, *J. Biotechnol.* **131**, 286 (2007).
- <sup>32</sup>N. N. Ye, J. H. Qin, W. W. Shi, X. Liu, and B. C. Lin, *Lab Chip* **7**, 1696 (2007).
- <sup>33</sup>J. L. Fu, Q. Fang, T. Zhang, X. H. Jin, and Z. L. Fang, *Anal. Chem.* **78**, 3827 (2006).
- <sup>34</sup>S. L. Zhou, Q. X. Dong, S. N. Li, J. F. Gu, X. X. Wang, and G. Zhu, *Aquat. Toxicol.* **95**, 339 (2009).
- <sup>35</sup>C. B. Kimmel, W. W. Ballard, S. R. Kimmel, B. Ullmann, and T. F. Schilling, *Dev. Dyn.* **203**, 253 (1995).
- <sup>36</sup>See supplementary material at <http://dx.doi.org/10.1063/1.3605509> for the development and exposed toxicity of embryonic zebrafish (Figs. S11–S17).
- <sup>37</sup>N. N. Ye, J. H. Qin, W. W. Shi, and B. C. Lin, *Electrophoresis* **28**, 1146 (2007).
- <sup>38</sup>E. Shang and R. Wu, *Environ. Sci. Technol.* **38**, 4763 (2004).
- <sup>39</sup>N. Bhattacharjee and A. Folch, Proceedings of MicroTAS 2010 Conference, 2010 (unpublished), p. 1688.
- <sup>40</sup>S. Sugiura, K. Hattori, and T. Kanamori, Proceedings of MicroTAS 2009 Conference, 2009 (unpublished), p. 27.
- <sup>41</sup>W. Dai, Y. Z. Zheng, K. Q. Luo, and H. K. Wu, *Biomicrofluidics* **4**, 024101 (2010).
- <sup>42</sup>J. H. Kang and J. K. Park, *Sens. Actuators B* **107**, 980 (2005).
- <sup>43</sup>B. G. Chung and J. Choo, *Electrophoresis* **31**, 3014 (2010).
- <sup>44</sup>H. A. Yusuf, S. J. Baldock, R. W. Barber, P. R. Fielden, N. J. Goddard, S. Mohr and B. Brown, *Lab Chip* **9**, 1882 (2009).
- <sup>45</sup>B. A. Mendelsohn, B. L. Kassebaum, and J. D. Gitlin, *Dev. Dyn.* **237**, 1780 (2008).
- <sup>46</sup>P. A. Padilla and M. B. Roth, *Proc. Natl. Acad. Sci. U.S.A.* **98**, 7331 (2001).
- <sup>47</sup>G. A. Giridharan, M. D. Nguyen, R. Estrada, V. Parichehreh, T. Hamid, M. A. Ismahil, S. D. Prabhu, and P. Sethu, *Anal. Chem.* **82**, 7581 (2010).
- <sup>48</sup>G. Gellert and J. Heinrichsdorff, *Water Res.* **35**, 3754 (2001).
- <sup>49</sup>B. Kalyanaraman, J. Joseph, S. Kalivendi, S. Wang, E. Konorev, and S. Kotamraju, *Mol. Cell. Biochem.* **234/235**, 119 (2002).
- <sup>50</sup>P. K. Singal, T. Li, D. Kumar, I. Danelisen, and N. Iliskovic, *Mol. Cell. Biochem.* **207**, 77 (2000).
- <sup>51</sup>L. Saint-Amant and P. Drapeau, *J. Neurobiol.* **37**, 622 (1998).
- <sup>52</sup>D. S. Antkiewicz, C. G. Burns, S. A. Carney, R. E. Peterson, and W. Heideman, *Toxicol. Sci.* **84**, 368 (2005).
- <sup>53</sup>C. C. Lin, M. Hui, and S. H. Cheng, *Toxicol. Appl. Pharmacol.* **222**, 159 (2007).
- <sup>54</sup>K. C. Brannen, J. M. Panzica-Kelly, T. L. Danberry, and K. A. Augustine-Rauch, *Birth Defects Res. C* **89**, 66 (2010).
- <sup>55</sup>M. M. Crane, K. Chung, J. Stirman, and H. Lu, *Lab Chip* **10**, 1509 (2010).